Effect of the Molecular Chains Grafted on Graphene Nanosheets on the Properties of Poly(L-lactic acid) Nanocomposites

Lei Chen, Xianhua Li, Liyuan Wang, Wei Wang, Zhiwei Xu
Key Laboratory of Advanced Braided Composites, Ministry of Education, School of Textiles, Tianjin Polytechnic University, Tianjin 300160, People's Republic of China

We prepared thermally reduced graphene oxide (TRG) grafted with polymethyl methacrylate (PMMA) and polyvinyl acetate (PVAc) (TRG-g-PMMA and TRG-g-PVAc) by γ-ray irradiation-induced graft polymerization and studied their effects on poly(L-lactic acid) (PLLA) nanocomposites. PMMA and PVAc chains were proved to be grafted on the TRG surface successfully. TRG-*g*-PMMA and TRG-*g*-PVAc was found to restrict the crystallization behavior of PLLA compared with TRG. Moreover, tensile-test results showed that TRG-*g*-PMMA and TRG-*g*-PVAc could enhance the elongation at break of PLLA nanocomposites without reducing the tensile strength and modulus compared with TRG, which indicated that the grafting of PMMA and PVAc chains on TRG could improve the toughness of PLLA nanocomposites. POLYM. COMPOS., 38:5–12, 2017.

INTRODUCTION

The biodegradable polymers have been attracting attention due to the increasing environmental pollution problems and the limited availability of petrochemical resources [1]. Poly(L-lactic acid) (PLLA), a linear aliphatic thermoplastic polymer, is one of the most promising environmentally friendly biodegradable plastics [2], since its 100% biodegradable and high mechanical properties [3]. Nevertheless, its crystallization rate, thermal and mechanical properties need to be improved for long-term high performance application.

PLLA nanocomposites exhibit dramatic changes in some properties at very low loadings (generally $\leq$2 wt%) of nanofillers like carbon nanotubes (CNTs) [1, 4, 5], cellulose nanofibers [3, 6], hydroxyapatite [7], and graphene [8, 9]. Many reports have verified that the addition of nanomaterials can increase the crystallization rate, and promote the thermal stability and mechanical strength of PLLA. However, the optimal performance conferred by these nanofillers can be achieved only when the homogeneous dispersion of nanofillers and strong interfacial adhesion between nanofillers and polymer matrix are realized [10–12].

Graphene, a single-atom-thick sheet of hexagonally arrayed sp^2-bonded carbon, chemically similar to CNTs, and structurally analogs to silicate layers [13], has drawn the attention of researchers in various fields due to its remarkable mechanical, thermal [14], and electrical properties [15]. With such outstanding properties, graphene nanosheets can be usefully applied as a reinforcing material in PLLA. However, to improve the solubility of graphene nanosheets in various organic solvents, as well as their miscibility with PLLA, the preparation of graphene derivatives by chemical modification has been the subject of intense interest recently [16–18]. In our previous work [19], we have studied the properties of graphene oxide (GO) grafted with PLLA (GO-*g*-PLLA)/PLLA nanocomposite, searching the effect of the PLLA grafted on GO on the properties of PLLA. The results show that GO-g-PLLA enhanced the dispersion and interfacial interactions between GO and PLLA matrix and thus improved the final thermostability and mechanical properties of nanocomposites. Although the GO-*g*-PLLA was synthesized via one step based on *in situ* polycondensation of the L-lactic acid monomers initiated by lyophilized GO, the process still can cause the aggregation of GO and the chemical method is limited in quantities and not environmental.

Recently, γ-ray irradiation, as a controlled method for modifying the physical and chemical properties of carbon materials, has attracted much attention [20] due to being environmentally safe and simple to industrialize. It was shown that grafting and functionalization of carbon materials with polymers induced by γ-rays [21–23] enhanced their solubility. Jovanovic et al. [24] described γ-irradiation for highly efficient functionalization of CNTs

Correspondence to: Z. Xu; e-mail: xuzhiwei@tjpu.edu.cn
Contract grant sponsor: National Natural Science Foundation of China; contract grant number: U1362108, 11175130.
DOI 10.1002/pc.23553
Published online in Wiley Online Library (wileyonlinelibrary.com).

by DNA wrapping, and found that it significantly improved the dispersion of CNTs and the functionalization was stabilized by electrostatic forces. Guo et al. [23] irradiated CNTs with γ-rays to modified them with thionyl chloride and decylamine, enhancing the solubility of CNTs in acetone and tetrahydrofuran. Zhang et al. [22] decorated GO with poly(vinyl acetate) (PVAc) by γ-ray irradiation-induced graft polymerization. Chen et al. [25] found that graphite oxide can be successively intercalated, grafted and exfoliated in monomers by γ-ray irradiation to obtain functionalized graphene nanosheets. Generally, it was found that γ-ray irradiation presents a facile route for the preparation of dispersible graphene and shows great potential in the preparation of graphene-based composites by solution processes.

It is known that the compatibilization of PLLA can be achieved by addition of polymers which are miscible or partial miscible with PLLA [26]. Eguiburu et al. [27] and Zhang et al. [28] found that the blends of PLLA and polymethyl methacrylate (PMMA) showed a single glass-transition temperature, which indicated a miscible system of PLLA/PMMA. Jun et al. [29] found that the blends of PLLA and polyvinyl acetate (PVAc) also exhibited a single glass transition over the entire composition range, indicating that the blends were miscible systems. The monomers of PMMA and PVAc both have double bonds, so it is possible to functionalize the graphene with methyl methacrylate and vinyl acetate by γ-ray irradiation. And it could be anticipated that the functionalized graphene by γ-ray irradiation could exhibit excellent effects on reinforcing and toughening of PLLA.

In this work, we prepare thermally reduced graphene oxide (TRG), first, which have lots of defections on the surface. For strong interaction between TRG and hydrophobic polymer, we employed a facial strategy of γ-ray irradiation to functionalize TRG in monomers of PMMA and PVAc. The chemical structures of functionalized TRG are quantitatively identified using Fourier transform infrared (FT-IR), atomic force microscope (AFM) and thermogravimetric analysis (TGA). Finally, PLLA/functionalized-TRG composites are prepared. The effects of molecular chains on functionalized TRG on crystallization behaviors and thermal and mechanical properties of PLLA composites are examined in terms of the dispersion of functionalized TRG in PLLA matrix.

EXPERIMENTAL

Materials

Natural graphite powder was provided by Nanjing Xianfeng Nanomaterial Science and Technology, China. PLLA (4032D) was purchased from Nature Works. Other chemical reagents were purchased from Tianjin Reagents and used without further purification.

Preparation of TRG Powders

To prepare TRG, the pristine natural graphite was firstly oxidized with sulfuric acid (H_2SO_4), phosphoric acid (H_3PO_4), and potassium permanganate ($KMnO_4$) via the improved Hummers' method [30, 31]. In detail, a 9:1 mixture of concentrated H_2SO_4/H_3PO_4 (360:40 ml) was added to a mixture of graphite flakes (3.0 g, 1 wt equiv.) and $KMnO_4$ (18.0 g, 6 wt equiv.), producing a slight exotherm to 35–40°C. The reaction was then heated to 50°C and stirred for 12 h. The reaction was cooled to room temperature and poured on to ice (~400 ml) with 30% H_2O_2 (3 ml). Subsequently, the suspension of acid-treated graphite was washed with an aqueous hydrochloric acid solution (10 vol%) to remove the sulfate ions and then washed repeatedly with distilled water until pH = 7.The graphite oxide slurry was freeze-dried (−50°C) for 48 h and then vacuum-dried (45°C) for 48 h. Finally, TRG were obtained by the thermal-treatment of graphite oxide at 1,050°C for 30 s [32].

γ-Ray Radiation Induced Functionalization of TRG

The prepared TRG were dispersed in acetone thoroughly by sonication and a 10 mg/ml TRG dispersion was obtained. Then methyl methacrylate (MMA) was added to a concentration of 50% (v/v). The resultant mixture was deoxygenated by bubbling high-purity nitrogen through for 15 min and was then irradiated by γ-ray from a ^{60}Co source in an absorbed dose 100 kGy with 0.8 kGy/h dose rate at room temperature. After irradiation, the TRG–MMA mixture was purified repeatedly by cycling-membrane filtration/acetone-redispersion until no white emulsion precipitated when the filtrate was added to water. The precipitate was then dried in a vacuum oven at 50°C for 24 h to get TRG grafted with polymethyl methacrylate (PMMA) (TRG-*g*-PMMA). TRG grafted with polyvinyl acetate (PVAc) (TRG-*g*-PVAc) were also prepared with the same concentration as TRG-*g*-PMMA by the same procedure using vinyl acetate (VAc) as the monomer, ethyl acetate as the solvent and acetone as the purified solvent. The scheme of γ-ray radiation induced functionalization of TRG to prepare TRG-*g*-PMMA and TRG-*g*-PVAc is shown in Fig. 1.

Preparation of PLLA Nanocomposites. A predetermined amount of TRG-*g*-PMMA (0.5 wt%) was added to 200 ml chloroform and sonicated for 2 h, and then 20 g PLLA was added into the chloroform solutions, subsequently mixing for 3 h with mechanical stirring. The mixed solution of PLLA and TRG-*g*-PMMA was sonicated for another 2 h and then dried for 48 h at 55°C in a vacuum oven. In order to test the mechanical properties of the composites, rectangular samples were prepared by compression molding. The mold (100 mm × 100 mm × 1 mm) filled with the composite pellets was placed in hot press which was preheated at 170°C. A pressure of 20

 DOI 10.1002/pc

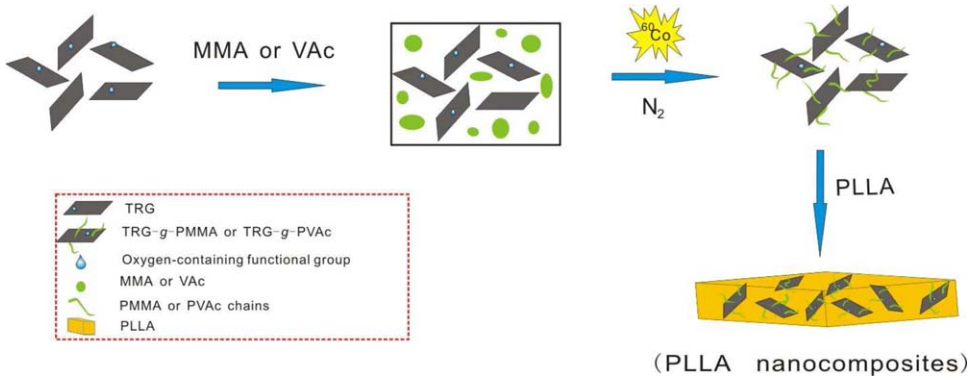

FIG. 1. The process of preparation of TRG-g-PMMA and TRG-g-PVAc and their PLLA composites. [Color figure can be viewed at wileyonlinelibrary.com]

MPa was applied for 2 min to soften the pellets and then a pressure of 40 MPa was applied for 10 min. Finally, the mold was quenched to 30°C with the cooled water recycle system and removed from the hot press to obtain a composite panel with 1 mm thickness. For comparison, PLLA, PLLA/TRG (0.5 wt%) and PLLA/TRG-*g*-PVAc (0.5 wt%) sheets were also prepared by the same method.

Instruments and Characterization

Atomic force microscopic (AFM) (Digital Instrument CSPM5500) measurements with the typical contact-mode were performed to observe the morphology of TRG, TRG-*g*-PMMA, and TRG-*g*-PVAc.

Fourier transform infrared spectroscopy (FTIR) and thermogravimetric analyses (TGA) were conducted to show the change of chemical character of TRG, TRG-*g*-PMMA, and TRG-*g*-PVAc. FTIR (Bruker Tensor 27) spectra were recorded from 400 to 4,000 cm^{-1} with a resolution of 2 cm^{-1} and 32 scans. TGA curves were obtained from a Mettler SDTA851e. The samples were heated from 30 to 800°C at a rate of 10°C/min in an aluminum crucible under 50 ml/min of nitrogen purging. The morphology and dispersion of TRG in the matrix were evaluated by a field-emission scanning electron microscope (FE-SEM) (JSM-6700F, accelerating voltage 10.0 kV). The tensile fractured surfaces of test specimens were sputter coated with gold before the SEM observations to avoid charging.

The crystallization behaviors and thermal characterizations of PLLA and nanocomposites were performed with a DSC 7 Perkin–Elmer instrument calibrated with indium under nitrogen atmosphere. Aluminum sample pans with ~3 mm diameter were used for all samples. The test samples were heated from 30 to 200°C at the rate of 10°C/min and held for 5 min at 200°C and eliminate the previous thermal history. They were then cooled to 30°C at 10°C/min and subsequently scanned from 30 to 200°C at 10°C/min again to study the effect of TRG and functionalization TRG of on the crystallization behavior and thermal properties of PLLA samples. Tensile properties of the nanocomposites were performed according to GB 1040.2 standard at the crosshead speed of 5 mm/min, on a universal mechanical testing machine (MTI INSTRON). Five measurements were carried out for each sample.

RESULTS AND DISCUSSION

Morphology and Chemical Characterizations of Nanofillers

Figure 2 shows the AFM photographs of TRG, TRG-*g*-PMMA, and TRG-*g*-PVAc. As expected, TRG presents an average thickness of 1.50 ± 0.20 nm before modification, while TRG-*g*-PMMA and TRG-*g*-PVAc show the higher thicknesses of 3.46 ± 0.21 and 3.03 ± 0.17nm, respectively. The increase of thickness can be attributed to the PMMA chains or PVAc chains on TRG surface. Thus it preliminarily showed that the PMMA and PVAc were grafted on the surface of TRG.

FTIR spectroscopy is used to observe the functional change of TRG with radiation treatment. The FTIR transmittance spectra of TRG before and after modification (TRG, TRG-*g*-PMMA, and TRG-*g*-PVAc) are shown in Fig. 3. The produced TRG exhibits three characteristic peaks at 3,431, 1,626, and 1,125 cm^{-1} indicating the O—H stretching vibrations, skeletal vibrations from unoxidized graphene domains and C—O stretching vibrations, respectively [33]. The difference between the spectra of TRG and TRG-g-PMMA is obvious at the peaks of 1,730 and 1,429 cm^{-1}, which are the O—C=O characteristic absorption bands and the C—H bending mode of PMMA [34]. The appearance of characteristic peaks corresponding to PMMA indicates that TRG is grafted by PMMA chains. In the spectrum of TRG-g-PVAc, there are some new peaks at 1,731 cm^{-1} (ν C=O), 1,431 cm^{-1} (δ_{as} CH_3), 1,230 cm^{-1} (ν O—C=O) and 928 cm^{-1} (δ C—H), which can be assigned as the characteristic peaks of PVAc [22]. Thus, it verifies that the PVAc chains are grafted to TRG.

The degree of grafting is estimated by TGA and is calculated using *Eq. 1* [25]:

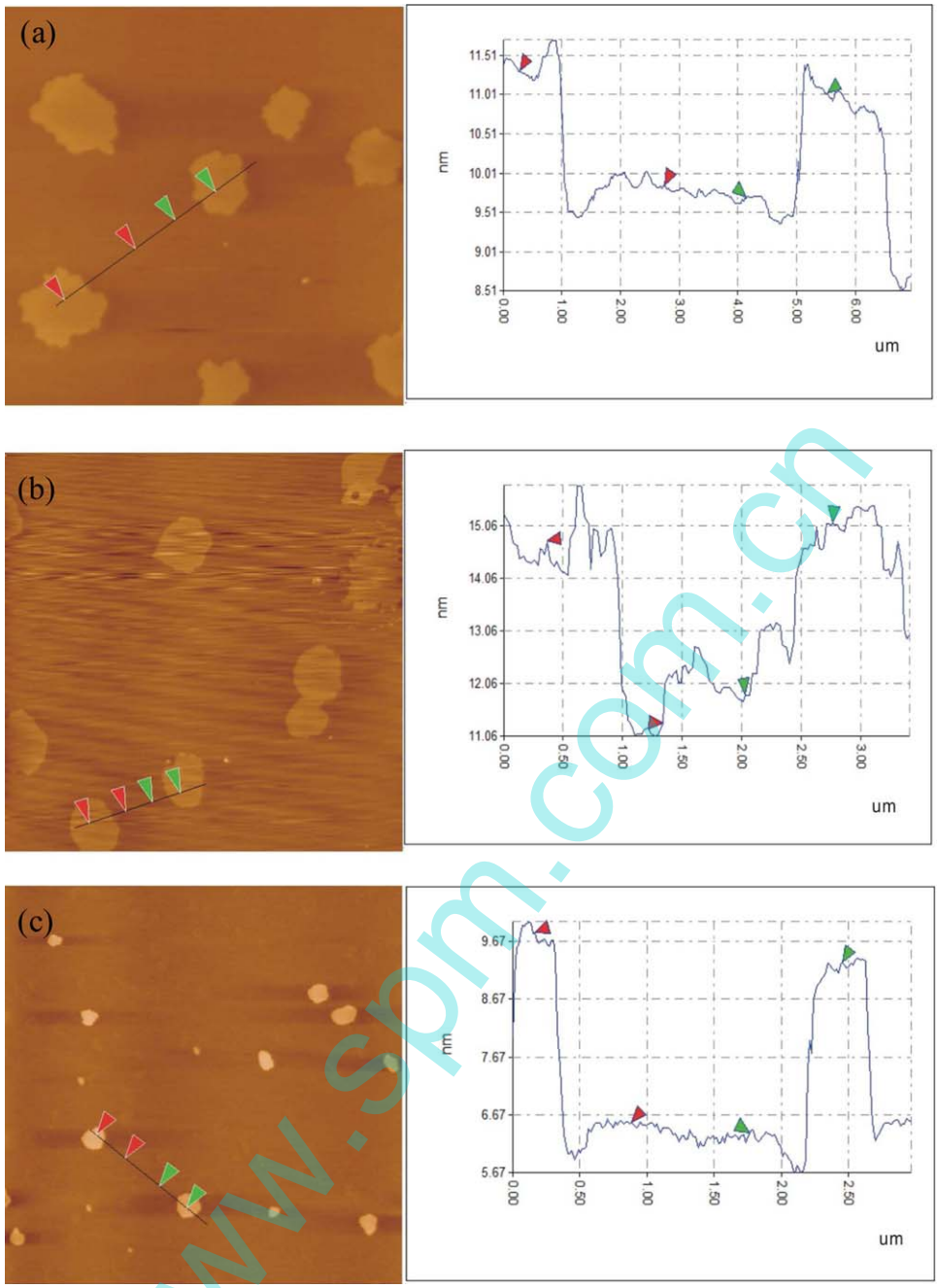

FIG. 2. Tapping mode AFM images of (a) TRG, (b) TRG-g-PMMA, and (c)TRG-g-PVAc. [Color figure can be viewed at wileyonlinelibrary.com]

$$\mathrm{DG}(\%) = \frac{R_G - R}{R_G - R_P} \times 100\% \quad (1)$$

wherein DG represents the degree of grafting, while R_G, R, and R_P represent the residual weight percentage(wt%) of TRG, TRG-*g*-PMMA, or TRG-*g*-PVAc and PMMA or PVAc, respectively. Figure 4 shows the TGA curves of TRG, TRG-*g*-PMMA, and TRG-*g*-PVAc in the temperature ranged from 30 to 800°C. TRG is thermally stable, and the residual weight percentage at 800°C is 87.4 wt%. TRG-*g*-PMMA has two clearly separated weight loss stages in the range of 30–100 and 200–410°C, which correspond to the removal of adsorbed water (2.6 wt%) and the decomposition of grafted PMMA [34, 35]. The residual weight percentage of TRG-*g*-PMMA at 800°C is shown as 53.3 wt% in Fig. 4, which is actually 55.7% without regarding the removal of absorbed water. As for TRG-g-PVAc, there are three clearly separated weight loss stages in the range of 30–100, 220–360, and 380–470°C, which correspond to the removal of adsorbed water (2.3 wt%) and decomposition of the grafted PVAc [22, 36]. The residual weight percentage is 54.0 wt%. Assuming the grafted polymer chains were completely PMMA or PVAc, the weight percentage of grafted

 DOI 10.1002/pc

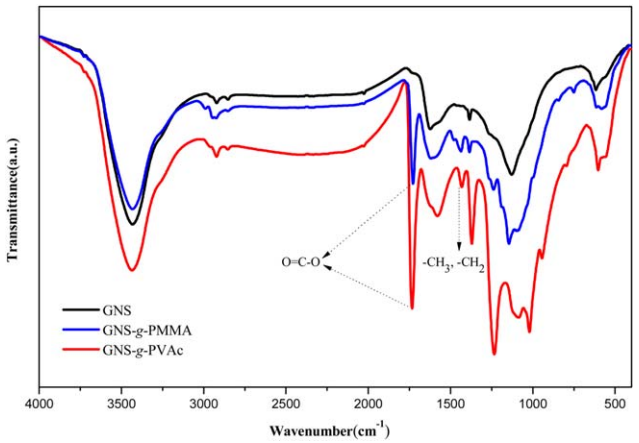

FIG. 3. FTIR spectra of TRG, TRG-g-PMMA, and TRG-g-PVAc. [Color figure can be viewed at wileyonlinelibrary.com]

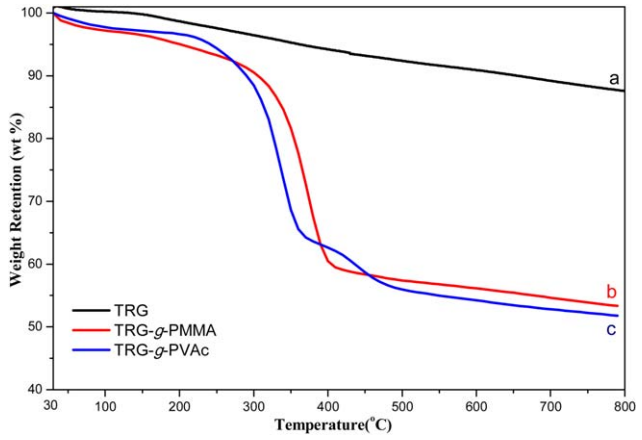

FIG. 4. Thermal degradation curves of (a) TRG, (b)TRG-*g*-PMMA, and (c) TRG-g-PVAc. [Color figure can be viewed at wileyonlinelibrary.com]

PMMA and PVAc chains was as high as 36.2 and 38.2 wt%, respectively, as calculated according to *Eq. 1*.

The Dispersity of Nanofillers in Organic Solvent and PLLA Nanocomposites. The dispersity of TRG, TRG-*g*-PMMA, and TRG-*g*-PVAc in chloroform was tested by a sedimentation experiment. As seen in Fig. 5a, both of them could form homogeneous solutions (0.5 mg/ml) after sonication for 2 h. However, TRG was precipitated at the bottom after 24 h of standing, while TRG-*g*-PMMA and TRG-*g*-PVAc were still well dispersed in the solution (Fig. 5b). This difference resulted from the grafted molecular chains which have a strong interaction with the solvent, thus facilitating a good dispersion of them in chloroform.

To characterize the morphology and dispersity of nanofillers in the nanocomposites, FE-SEM images of fracture surfaces of PLLA, PLLA/TRG, PLLA/TRG-g-PMMA, and PLLA/TRG-*g*-PVAc composites were examined, as displayed in Fig. 6. The PLLA showed a smooth fracture surface morphology (Fig. 6a). For PLLA/TRG nanocomposites, it showed a rougher surface than PLLA. However, we can see that a part of TRG formed agglomeration in the PLLA matrix (Fig. 6b). It is believed that TRG aggregations in the PLLA matrix were caused by the Van der Waals interaction among TRG as well as the poor compatibility of TRG with the PLLA matrix. In the case of PLLA/TRG-g-PMMA, and PLLA/TRG-g-PVAc nanocomposites, the fracture surfaces of them were relatively crude, which indicated that more energy was required to break the composites and the functionalized TRG formed strong interface with PLLA. In addition, the fracture surface of PLLA/functionalized TRG did not show noticeable TRG aggregations due to the molecular chains wrapped around TRG which supported TRG to mix well with PLLA matrix.

Crystallization Behavior of the Samples. The crystallization behaviors and thermal characterizations of PLLA and PLLA nanocomposites were investigated with DSC. Figure 7 shows the thermograms of DSC in second heating scans for PLLA and PLLA nanocomposites, which indicated the degree of crystallinity (χ_c) and thermal characterizations of PLLA samples. The χ_c of the samples were calculated using *Eq. 2* [37].

$$\chi c\,(\%) = \frac{\Delta H\mathrm{m} - \Delta H\mathrm{c}}{\Delta H0} \times 100\% \qquad (2)$$

wherein ΔH_m and ΔH_c represent the melting enthalpy and cold crystallization enthalpy of the samples, respectively. ΔH_0 represent the melting enthalpy of 100% crystalline PLLA (93 J/g).

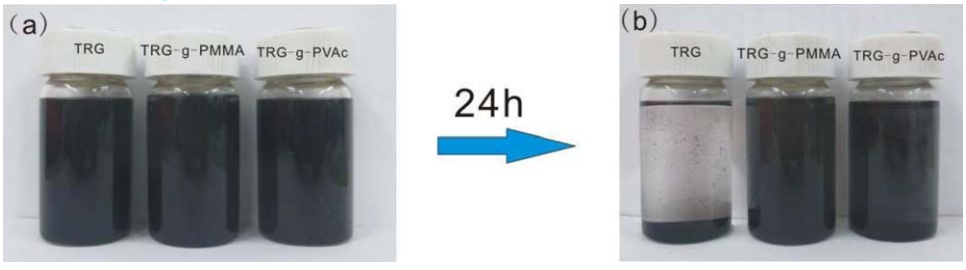

FIG. 5. (a) Photos of TRG, TRG-*g*-PMMA, and TRG-*g*-PVAc dispersion in chloroform (0.5 mg/ml) after sonication for 2 h; and (b) states after standing for 24 h. [Color figure can be viewed at wileyonlinelibrary.com]

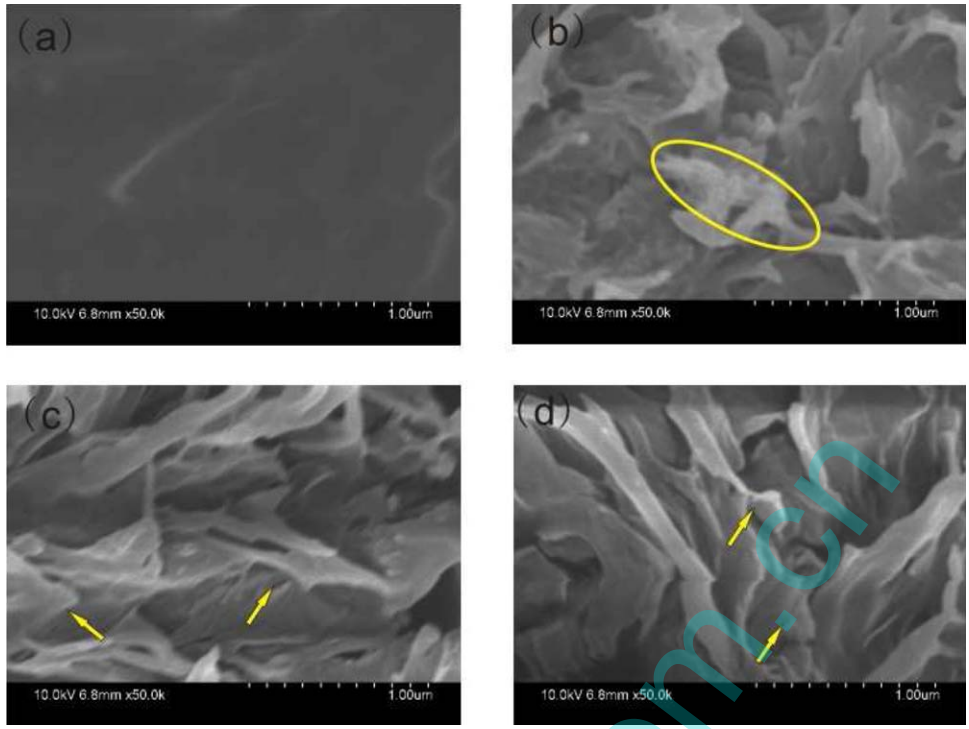

FIG. 6. Tensile fracture surface of (a) PLLA; (b) PLLA/TRG; (c) PLLA/TRG-*g*-PMMA; (d) PLLA/TRG-*g*-PVAc. [Color figure can be viewed at wileyonlinelibrary.com]

The T_g, T_{cc}, T_m, ΔH_c, ΔH_m, and χ_c of the PLLA samples which had eliminated the previous thermal history in the first heating were summarized in Table I. T_g of the PLLA nanocomposites were found to be increased from ~63.3 to ~63.7°C than neat PLLA in Table I, which was seemed to be negligible. However, a new interface was introduced into the polymers by adding nanofillers, which may decrease the thermal properties of nanofillers. Thus, the addition of TRG fillers into polymers constrains the segmental motion of the PLLA chains, which overcomes the negative effect of the new interface and brings the slight increase of T_g. For PLLA/TRG, the attachment between PLLA and TRG may be caused by hydrogen bonding and electrostatic attraction, as demonstrated in other reports [38]. For PLLA/TRG-*g*-PMMA and PLLA/TRG-*g*-PVAc, the attachment should be caused by the chemical bonding effect between PLLA chains and chains grafted on TRG. On the other hand, the T_{cc} of PLLA nanocomposites were lower than that of neat PLLA, which indicated that the addition of graphene nanosheets could improve the cool crystallization behavior of PLLA, especially the addition TRG and TRG-*g*-PMMA. The phenomenon is corresponded to the appearance of melt crystallization peaks of PLLA/TRG and PLLA/TRG-*g*-PMMA in cooling scan as shown in Fig. 5a. Finally, the χ_c of the PLLA samples were calculated to study the effect of nanofillers on the crystallization property of PLLA. As seen in Table I, the χ_c of neat PLLA (1.92%) was improved to 9.29, 8.15, and 3.72% after the addition of TRG, TRG-*g*-PMMA, and TRG-*g*-PVAc, respectively. These results fully confirm that TRG behave as a

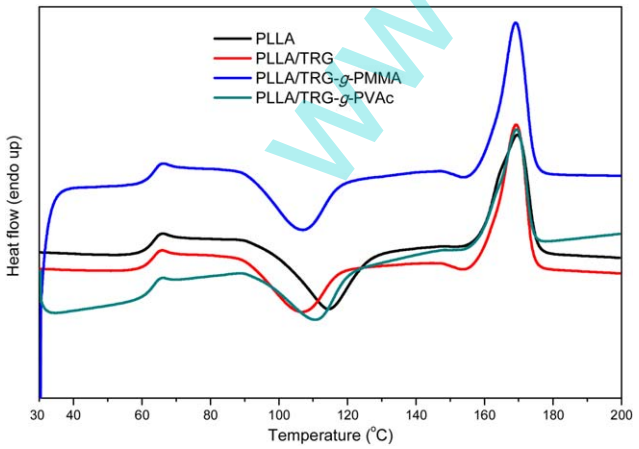

FIG. 7. Thermograms of DSC for PLLA and PLLA nanocomposites. [Color figure can be viewed at wileyonlinelibrary.com]

TABLE I. T_g, T_{cc}, T_m, ΔH_c, ΔH_m, and χ_c of the samples in second heating scans.

Samples	T_g (°C)	T_{cc} (°C)	T_m (°C)	ΔH_c (J/g)	ΔH_m (J/g)	χ_c (%)
PLLA	63.3	114.4	169.6	30.05	31.84	1.92
PLLA/EG	63.7	106.9	169.2	22.44	31.09	9.29
PLLA/EG-*g*-PMMA	63.6	107.1	169.1	23.82	31.41	8.15
PLLA/EG-*g*-PVAc	63.8	110.5	169.4	22.12	25.58	3.72

DOI 10.1002/pc

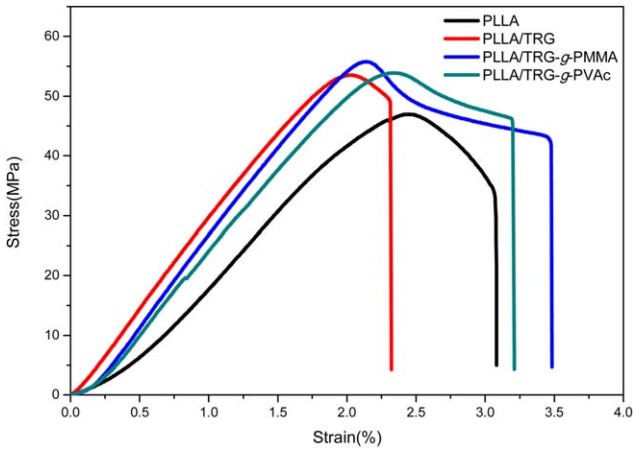

FIG. 8. Typical tensile stress–strain curves of PLLA, PLLA/TRG, PLLA/TRG-g-PMMA, and PLLA/TRG-g-PVAc nanocomposites. [Color figure can be viewed at wileyonlinelibrary.com]

remarkable nucleating agent for PLLA as reported elsewhere [39]. After grafting PMMA or PVAc chains, the long polymer chain molecular stretch into the PLLA matrix, limited the nucleating function of TRG, and reduced the χ_c of PLLA/GNA-*g*-PMMA and PLLA/TRG-*g*-PVAc. Besides, the amorphous PMMA [28] and PVAc [29] restrict the crystallization of PLLA, and thus the χ_c of PLLA/GNA-*g*-PMMA and PLLA/TRG-*g*-PVAc were lower than PLLA/TRG. While due to the existence of TRG, the χ_c values of them were still higher than neat PLLA.

Mechanical Properties of PLLA and Nanocomposites

Figure 8 shows the typical stress–strain curves of PLLA and the nanocomposites. The mean values and standard deviations of the mechanical properties of PLLA and nanocomposites are summarized in Table II. The figures clearly show that both tensile modulus and strength of PLLA were improved with the addition of TRG and its derivatives, while the strain at break of PLLA/TRG was decreased and that of PLLA/TRG-*g*-PMMA and TRG-*g*-PVAc basically had no variation compared with neat PLLA. The tensile strengths and Young's modulus of neat PLLA were increased by adding outstanding mechanical properties of graphene and good interfacial adhesion between PLLA and nanofillers.

As seen in many reports, the addition of TRG could increase the tensile strengths and Young's modulus of PLLA due to the reinforcing effect of graphene, and the decrease of the strain at break was owing to the hardening effect of TRG in the PLLA matrix [9, 40]. As for TRG-*g*-PMMA and TRG-*g*-PVAc nanocomposites, the tensile strength and Young's modulus were similar to PLLA/TRG, while the strains at break of them were increased from 2.3% of PLLA/TRG to about 2.7% and basically reached the value of neat PLLA. These could be explained by the fact that the molecular chains grafted on TRG (PMMA and PVAc) are miscible with PLLA [28, 29], which improved the mechanical interlock effect between nanofillers and matrix. The miscible systems improved the slipping effect between molecular chains and alleviated the hardening effect of TRG. It is predicted that higher concentration of miscible molecular chains attached on TRG will future improve the fracture toughness of PLLA.

TABLE II. Absolute value of tensile strength, tensile modulus, and elongation at break of PLLA samples.

Samples	Tensile strength[a] (MPa)	Tensile modulus (GPa)	Strain at break (%)
PLLA	46.8 ± 2.6	2.1 ± 0.3	2.8 ± 0.3
PLLA/TRG	53.6 ± 1.0	2.9 ± 0.2	2.3 ± 0.4
PLLA/TRG-*g*-PMMA	55.6 ± 1.3	2.6 ± 0.2	2.7 ± 0.2
PLLA/TRG-*g*-PVAc	53.0 ± 2.4	2.7 ± 0.3	2.8 ± 0.3

[a]Maximum stress.

CONCLUSIONS

The TRG was covalently functionalized with PMMA and PVAc by γ-ray irradiation-induced graft polymerization. TGA results showed that TRG could obtain a high grafting rate of PMMA and PVAc (about 37%). Moreover, PLLA, PLLA/TRG, PLLA/TRG-*g*-PMMA, and PLLA/TRG-*g*-PVAC nanocomposites were prepared to investigate the effect of TRG and functionalized TRG on the crystallization, thermal and mechanical properties of PLLA. The results showed that the molecular chains grafted on TRG could improve the dispersion of TRG in the organic solvent and thus improved the dispersion in PLLA matrix. The thermograms of DSC indicated that the addition of TRG and functionalized TRG both improved the degree of crystallinity and thermostability of PLLA. After grafting with PMMA or PVAc molecular chain, the nucleating property of TRG was restricted due to the long polymer chain molecular which stretched into the PLLA matrix. Tensile test results showed that TRG-*g*-PMMA and TRG-*g*-PVAc could enhance the elongation at break of PLLA nanocomposites without reducing the tensile strength and modulus, which indicated the improvement of PLLA toughness by introducing the TRG grafted with PMMA or PVAc chains. As one of the most efficient and environmental method to prepare functionalized graphene, radiation techniques should be favored in industrialization and the effect of molecular chains grafted on graphene on the graphene nanocomposites should be further studied.

ACKNOWLEDGMENTS

The work was funded by the National Natural Science Foundation of China (U1362108, 11175130).

REFERENCES

1. C.C. Teng, C.C.M. Ma, B.D. Cheng, Y.F. Shih, J.W. Chen, and Y.K. Hsiao, *Compos. A*, **42**, 928 (2011).
2. C.Y. Hung, D.K. Huang, C.C. Wang, and C.Y. Chen, *J. Inorg. Organomet. Polym. Mater.*, **23**, 1389 (2013).
3. M.K.M. Haafiz, A. Hassan, Z. Zakaria, I.M. Inuwa, M.S. Islam, and M. Jawaid, *Carbohydr. Polym.*, **98**, 139 (2013).
4. S. Barrau, C. Vanmansart, and M. Moreau, *Macromolecules*, **44**, 6496 (2011).
5. G.M. Neelgund and A. Oki, *Appl. Catal. A: Gen.*, **399**, 154 (2011).
6. T. Wang and L.T. Drzal, *ACS Appl. Mater. Interface*, **4**, 5079 (2012).
7. Z.K. Hong, P.B. Zhang, C.L. He, X.Y. Qiu, A.X. Liu, L. Chen, X. Chen, and X. Jeng, *Biomaterials*, **26**, 6296 (2005).
8. Y. Cao, J. Feng, and P. Wu, *Carbon*, **48**, 3834 (2010).
9. C. Bao, L. Song, W. Xing, B. Yuan, C.A. Wilkie, J. Huang, Y. Guo, Y. Hu, *J. Mater. Chem.*, **22**, 6088 (2012).
10. M. Tait, A. Pegoretti, A. Dorigato, and K. Kalaitzidou, *Carbon*, **49**, 4280 (2011).
11. P.G. Seligra, F. Nuevo, M. Lamanna, and L. Famá, *Compos. B*, **46**, 61 (2013).
12. J.T. Yoon, S.C. Lee, and Y.G. Jeong, *Compos. Sci. Technol.*, **70**, 776 (2010).
13. K. Wakabayashi, C. Pierre, D.A. Dikin, R.S. Ruoff, T. Ramanathan, L.C. Brinson, J.M. Torkelson, *Macromolecules*, **41**, 1905 (2008).
14. S. Stankovich, D.A. Dikin, G.H. Dommett, K.M. Kohlhaas, E.J. Zimney, E.A. Stach, R.D. Piner, S.T. Nguyen, R.S. Ruoff, *Nature*, **442**, 282 (2006).
15. A.H. Castro Neto, F. Guinea, N.M.R. Peres, K.S. Novoselov, and A.K. Geim, *Rev. Mod. Phys.*, **81**, 109 (2009).
16. P. Steurer, R. Wissert, R. Thomann, and R. Mulhaupt, *Macromol. Rapid Commun.*, **30**, 316 (2009).
17. L. Hua, W. Kai, J. Yang, and Y. Inoue, *Polym. Degrad. Stabil.*, **95**, 2619 (2010).
18. J.H. Yang, S.H. Lin, and Y.D. Lee, *J. Mater. Chem.*, **22**, 10805 (2012).
19. W. Li, Z. Xu, L. Chen, M. Shan, X. Tian, C. Yang, H. Lv, X. Qian, *Chem. Eng. J.*, **237**, 291 (2014).
20. Z. Xu, L. Chen, L. Liu, X. Wu, and L. Chen, *Carbon*, **49**, 350 (2011).
21. L. Chen, Z. Xu, J. Li, X. Wu, and L. Chen, *Adv. Mater. Res.*, **79–82**, 497 (2009).
22. B. Zhang, Y. Zhang, C. Peng, M. Yu, L. Li, B. Deng, P. Hu, C. Fan, J. Li, Q. Huang, *Nanoscale*, **4**, 1742 (2012).
23. J. Guo, Y. Li, S. Wu, and W. Li, *Nanotechnology*, **16**, 2385 (2005).
24. S.P. Jovanovic, Z.M. Markovic, D.N. Kleut, N.Z. Romcevic, V.S. Trajkovic, M.D. Dramicanin, B.M.T. Markovic, *Nanotechnology*, 20 (2009).
25. L. Chen, Z. Xu, J. Li, Y. Li, M. Shan, C. Wang, Q. Guo, L. Liu, G. Chen, *J. Mater. Chem.*, **22**, 13460 (2012).
26. H.T. Oyama, *Polymer*, **50**, 747 (2009).
27. J.L. Eguiburu, J.J. Iruin, M.J. Fernandez-Berridi, and J.S. Roman, *Polymer*, **39**, 6891 (1998).
28. G.B. Zhang, J.M. Zhang, S.G. Wang, and D.Y. Shen, *J. Polym. Sci. Part B: Polym. Phys.*, **41**, 23 (2003).
29. J.W. Park and S.S. Im, *Polymer*, **44**, 4341 (2003).
30. D.C. Marcano, D.V. Kosynkin, J.M. Berlin, A. Sinitskii, Z. Sun, A. Slesarev, L.B. Alemany, *ACS Nano*, **4**, 4806 (2010).
31. C. Shi, L. Chen, Z. Xu, Y. Jiao, Y. Li, C. Wang, M. Shan, Z. Wang, Q. Guo, *Phys. E*, **44**, 1420 (2012).
32. H.C. Schniepp, J.L. Li, M.J. McAllister, H. Sai, M. Herrera-Alonso, D.H. Adamson, R.K. Prud'homme, R. Car, D.A. Saville, I.A. Aksay, *J. Phys. Chem. B*, **110**, 8535 (2006).
33. K. Liu, L. Chen, Y. Chen, J. Wu, W. Zhang, F. Chen, Q. Fu, *J. Mater. Chem.*, **21**, 8612 (2011).
34. L. Lei, J. Qiu, and E. Sakai, *Chem. Eng. J.*, **209**, 20 (2012).
35. J. Wang, Z. Shi, Y Ge, Y. Wang, J. Fan, and J. Yin, *J. Mater. Chem.*, **22**, 17663 (2012).
36. S. Zulfiqar and S. Ahmad, *Polym. Degrad. Stab.*, **71**, 299 (2001).
37. P.H. Nam, P. Maiti, M. Okamoto, T. Kotaka, N. Hasegawa, A. Usuki, *Polymer*, **42**, 9633 (2001).
38. L. He, J. Sun, X. Wang, X. Fan, Q. Zhao, L. Cai, R. Song, Z. Ma, *Mater. Chem. Phys.*, **134**, 1059 (2012).
39. M. Murariu, A.L. Dechief, L. Bonnaud, Y. Paint, A. Gallos, G. Fontaine, S. Bourbigot, P. Dubois, *Polym. Degrad. Stabil.*, **95**, 889 (2010).
40. I.H. Kim and Y.G. Jeong, *J. Polym. Sci. Part B: Polym. Phys.*, **48**, 850 (2010).

DOI 10.1002/pc